 doi:10.20944/preprints202012.0678.v1

Article

Effects of MOVPE Growth Conditions on GaN Layers Doped with Germanium

Dario Schiavon [1,*], Elżbieta Litwin-Staszewska [1], Rafał Jakieła [2], Szymon Grzanka [1], Piotr Perlin [1]

[1] Institute of High Pressure Physics of the Polish Academy of Sciences (IWC-PAN), al. Sokołowska 29/37, 01-142 Warsaw, Poland; dyrekcja@unipress.waw.pl
[2] Institute of Physics of the Polish Academy of Sciences (IF-PAN), al. Lotników 32/46, 02-668 Warsaw, Poland; director@ifpan.edu.pl
* Correspondence: dario.schiavon@unipress.waw.pl

Abstract: The effect of growth temperature and precursor flows on the doping level and surface morphology of Ge-doped GaN layers was researched. The results show that germanium is more readily incorporated at low temperature, high growth rate and high V/III ratio, thus revealing a similar behavior to what was previously observed for indium. V-pit formation can be blocked at high temperature but also at low V/III ratio, the latter of which however causing step bunching.

Keywords: Ge; germanium; doping; GaN; gallium; nitride; MOVPE; epitaxy

1. Introduction

In the last few years there has been a renewed interest in highly doped *n*-GaN layers produced by metal-organic vapor-phase epitaxy (MOVPE). Such layers are very important for the optimization of the operative voltage of GaN-based electronic devices, especially those with tunnel junctions [1], as well as for a better control of the layers' refractive index thanks to the plasmonic effect [2]. For all these applications, it is desirable to reach higher doping levels than those achievable with silicon as a donor impurity. In fact, silicon proved inadequate at providing a doping level higher than 10^{19} cm^{-3} because of a general deterioration of the surface morphology [3] probably caused by the antisurfactant property of Si [4]. Recently, germanium has emerged as a better alternative to silicon as a donor dopant. While it has a similar activation energy [5,6] and provides similar carrier mobility at every doping level [7], germanium has proved capable of attaining doping levels beyond 10^{20} cm^{-3} without negatively affecting the surface morphology [3,8]. Such a high doping level is sufficient to bring about a decrease of the refractive index of the material and opens up possibilities of using GaN layers as waveguide claddings in laser structures [2,9].

One problematic aspect of GaN:Ge (i.e. Ge-doped GaN) growth is that the incorporation efficiency of germanium depends strongly on the MOVPE growth conditions. For example, Fritze et al. [3] reported that their dopant precursor flow for germanium was 2–3 orders of magnitude higher than for silicon at the same resulting doping level. Specifically, for a doping level of 1.9×10^{20} cm^{-3}, their Ge/Ga precursor ratio was probably as high as 1/3 in the gas phase. However, Kirste et al. [10] obtained a similar Ge-doping level with a Ge/Ga precursor ratio that is two orders of magnitude lower, and therefore quite similar to conventional Si doping. The incertainty about the incorporation efficiency makes it difficult to control the doping level appropriately, and is therefore an interesting subject of study.

Another challenge of GaN:Ge growth is the difficulty of avoiding the formation of V-pits (hexagonal inverse-pyramidal pits). Such morphological defects have longtime been known to form at low growth temperature, such as in the case of InGaN layers (650–850 °C), on top of screw (or mixed) dislocations [11]. During the growth of GaN:Ge layers, however, these can be produced at temperatures as high as 1075 °C [3], depending possibly also on the concentration of the incorporated

Preprints (www.preprints.org) | NOT PEER-REVIEWED | Posted: 28 December 2020 doi:10.20944/preprints202012.0678.v1

Table 1. Summary of the growth conditions and characterization results of the first series of samples, where only the growth temperature and the TMGa flow were varied. The [Ge] column shows the concentration of germanium impurities in the test layers as measured by SIMS. The n and μ columns show the electron density and mobility from the Hall-effect measurements.

Id	T (C)	GR ($\frac{m}{h}$)	NH_3 (slm)	TMGa ($\frac{mol}{min}$)	GeH_4 ($\frac{mol}{min}$)	[Ge] (cm^{-3})	n (cm^{-3})	μ ($\frac{cm^2}{Vs}$)
a	1008	3.09	2	80	7.6	$3–5 \times 10^{19}$	3.9×10^{19}	116
b	1026	2.97	2	80	7.6		1.6×10^{19}	145
c	1044	2.78	2	80	7.6		7.1×10^{18}	187
d	1062	2.65	2	80	7.6		4.2×10^{18}	218
e	1071	2.51	2	80	7.6		2.8×10^{18}	203
f	991	0.83	2	25	7.6		4.4×10^{19}	153
g	1016	0.73	2	25	7.6	$1–2 \times 10^{19}$	1.7×10^{19}	147
h	1037	0.60	2	25	7.6		7.3×10^{18}	205
i	1008	0.19	2	12	7.6	$1–2 \times 10^{19}$	1.1×10^{19}	224
j	1014	0.05	2	6	7.6	$3–7 \times 10^{18}$		

germanium. The physical mechanism proposed to explain their formation involves the segregation of liquid germanium droplets on top of screw dislocations. V-pits are then formed as a consequence of the disturbance provoked by the droplets themselves [12,13]. Different strategies have been proposed to clear the surface of V-pits, including reducing the density of screw dislocations [3] or, particularly in the case of hydride vapor-phase epitaxy (HVPE), reducing the partial pressure of diatomic hydrogen in the reactor chamber [12].

Until today, there has not yet been a systematic investigation detailing how the growth conditions affect germanium incorporation and V-pit formation. This article provides data showing that germanium incorporation behaves similarly to indium incorporation, suggesting that the underlying physical mechanism is the same, and additionally presents an alternative solution to the issue of V-pit formation.

2. Effect of temperature and TMGa flow

A starting series of ten samples, conveniently labelled with the letters "a"–"j", were grown at different temperatures and Ga-precursor flows on sapphire substrates by metal-organic vapor-phase epitaxy (MOVPE) in an Aixtron close-coupled-showerhead reactor. For all samples, the growth pressure was kept at 100 mbar, the showerhead gap at 6 mm and the total gas flow into the reactor at 8 slm using H_2 as carrier gas. The precursor gases are ammonia (NH_3), trimethylgallium (TMGa) and germane (GeH_4), the latter being supplied from a mix of 10% GeH_4 and 90% H_2 of 6-nine purity. For all samples, the NH_3 flow was kept at 2 slm and the GeH_4 flow at 7.6 mol/min, which is almost the minimum allowed by our dedicated mass-flow controller. The epitaxial structure consists of a 5-m-thick undoped GaN buffer layer, and a GaN:Ge test layer with thickness in the range 0.5–1.2 m. The growth rate (GR) was monitored by a laser reflectometer and the susceptor surface temperature (T) was measured by an Aixtron Argus^{TM} dual-wavelength pyrometer with emissivity correction. The samples were characterized by secondary-ion mass spectrometry (SIMS) and Van-der-Pauw Hall-effect measurements. The results are summarized in Table 1. Note that not all samples were measured by SIMS, and that sample "j" was highly resistive so it could not be characterized by Hall effect. However, wherever both types of data are available, we see that the electron density matches the germanium concentration within the uncertainty of the SIMS measurement, which is in agreement with the general expectation that germanium dopant is mostly activated at room temperature [5,6,14].

Figure 1 shows the GR and the electron density (from Hall measurements) as a function of temperature. The GR depends on the TMGa flow, of course, but it also depends on the temperature. The temperature dependence of the GR is a known phenomenon that is possibly caused by a combination

Preprints (www.preprints.org) | NOT PEER-REVIEWED | Posted: 28 December 2020 doi:10.20944/preprints202012.0678.v1

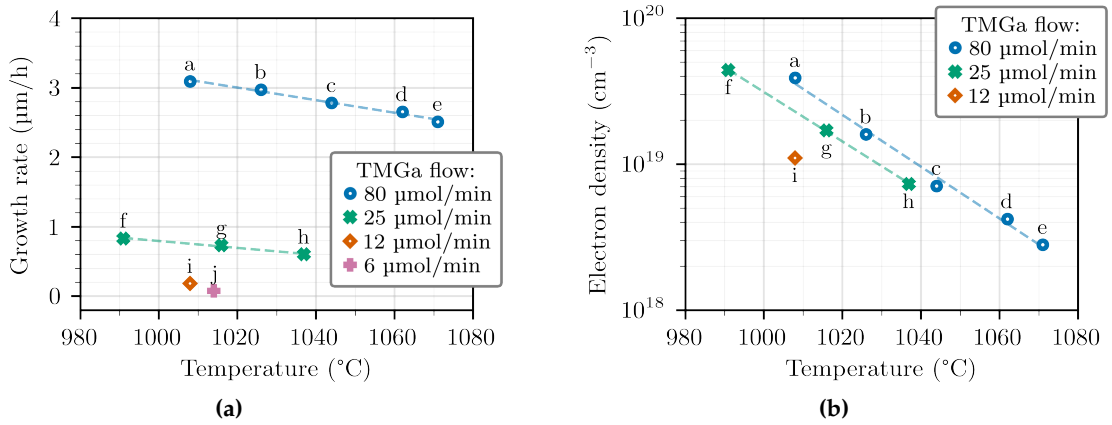

Figure 1. GR and electron density for GaN:Ge layers grown at different temperatures and TMGa flows, while the NH_3 and GeH_4 flows are kept at 2 slm and 7.6 mol/min, respectively. The dashed lines are linear fits to the data.

of parasitic reactions and thermal back-etching. Parasitic reactions are chemical reactions occurring in the gas phase among NH_3 and the metalorganic precursors, and producing dust particles that are quickly carried out of the reactor chamber with no interaction with the growth surface. In the case of III–nitride materials, parasitic reactions are especially well documented for the growth of AlGaN layers with TMGa and TMAl precursors [15]. Thermal back-etching, on the other hand, is the reverse reaction of growth itself and is caused by the breaking of the chemical bonds at the surface of the uppermost layer. It has been observed for GaN layers and it is known to be greatly enhanced by the presence of H_2 in the gas flow [16].

To better show which mechanism is prevailing in our case, we interpolated the GR corresponding to each TMGa flow at the temperature of 1010C. The resulting values are plotted in Figure 2. In addition to the Ge-doped samples, the plot also includes the GR of undoped GaN layers, which were grown in the exact same conditions except that no GeH_4 was introduced into the reactor. We note that the GR drops to zero for a TMGa flow close to 7 mol/min, which must be the flow at which the supply of ad-atoms from the precursors matches the loss due to back-etching. This clearly proves that back-etching is taking place. On the other hand, the same data exclude the possibility that parasitic reactions are occurring at these gas flows, because the relationship between GR and TMGa flow appears to be linear, whereas parasitic reactions would rather result in a drooping curve. We also note that GeH_4 does not have a significant influence on either the GR or the back-etching rate, because the corresponding lines on the plot do not have different slopes, nor do they have different intercepts against the x-axis. We cannot exclude, however, that parasitic reactions could become relevant at higher GeH_4 flows.

As for the concentration of germanium atoms in the layers, which we take to be equal to the electron density, it is clearly seen to decrease for increasing temperature independently of the TMGa flow. Besides, when comparing samples grown with different TMGa flows, given that the GeH_4 flow is unchanged, we would expect a sample grown with a lower TMGa flow to have a higher doping level, and therefore a higher electron density. However, this is not what is observed—the doping level decreases instead. In fact, our data indicate that the incorporation of germanium exhibits a similar behavior to the incorporation of indium in InGaN layers. In fact, indium is more easily incorporated at high GR and low temperature [17]. In the case of indium, this is commonly explained by the fact that indium ad-atoms desorb very easily from the growth surface due to the high vapor pressure of indium over (In)GaN [18]. In the case of germanium, given that we have already excluded the possibility of significant parasitic reactions, we can presume that the mechanism may be the same as it is for indium.

Preprints (www.preprints.org) | NOT PEER-REVIEWED | Posted: 28 December 2020 doi:10.20944/preprints202012.0678.v1

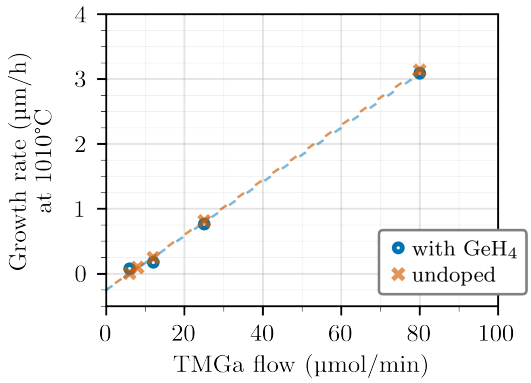

Figure 2. GR of Ge-doped and undoped GaN layers grown at 1010C with different TMGa flows. The GR of the doped layers is interpolated from the data of Figure 1a. Note that the data for doped and undoped layers overlap on the same line and that this line crosses the x-axis for a TMGa flow of 7 mol/min.

Table 2. Summary of the growth conditions and characterization results of the second series of samples, where the NH_3 flow is reduced to 0.5 slm. The [Ge] column shows the concentration of germanium impurities in the test layers as measured by SIMS. The n and μ columns show the electron density and mobility from the Hall-effect measurements.

Id	T (C)	GR ($\frac{m}{h}$)	NH_3 (slm)	TMGa ($\frac{mol}{min}$)	GeH_4 ($\frac{mol}{min}$)	[Ge] (cm^{-3})	n (cm^{-3})	μ ($\frac{cm^2}{V\,s}$)
k	970	0.50	0.5	25	45		1.3×10^{20}	100
l	970	0.67	0.5	25	18		1.8×10^{20}	90
m	976	0.81	0.5	25	7.6	$6–10 \times 10^{19}$	7.6×10^{19}	136
n	999	0.73	0.5	25	7.6		2.8×10^{19}	148

3. Effect of GeH_4 and NH_3 flow

The following series of samples (labelled "k"–"n", see Table 2) were grown with NH_3 flow reduced to 0.5 slm from the previous 2 slm. We consider at first samples "k"–"m", which are grown at approximately the same growth temperature of 970–976C but with variable GeH_4 flows. Their GR and electron density are shown in Figure 3. It is found that the electron density (and therefore the concentration of incorporated germanium) does not depend linearly on the GeH_4 flow, but instead peaks somewhere at about 15–30 mol/min and then decreases for increasing GeH_4 flow. Even this behavior, where the incorporation of a given species saturates and then starts to decrease for increasing precursor flow, has been observed for indium in InGaN layers [19,20]. In the case of indium, Guo et al. [20] have tentatively explained the decreasing trend after the peak as the effect of parasitic reactions. The same could be true for germanium since, even though we demonstrated that no parasitic reactions happen at the GeH_4 flow of 7.6 mol/min, we cannot exclude that parasitic reactions could be happening at the considerably higher flow of 45 mol/min (despite the slightly lower temperature of 970C). Assuming that these parasitic reactions involve both GeH_4 and TMGa as reagents, they can also explain the reduction of GR that is observed for increasing GeH_4 flows in Figure 3a.

It is also useful to compare the samples "f"–"h" from the first series with the samples "m"–"n" from the second series, which are grown with the same TMGa and GeH_4 flows but different NH_3 flows. Their GR and electron density is shown in Figure 4. Both the GR and the electron density are slightly lower in the second series with respect to the first series, when comparing at the same temperature. The fact that the incorporation of the more volatile group-III species is enhanced at high V/III ratio has also been confirmed for InGaN growth [20].

Preprints (www.preprints.org) | NOT PEER-REVIEWED | Posted: 28 December 2020 doi:10.20944/preprints202012.0678.v1

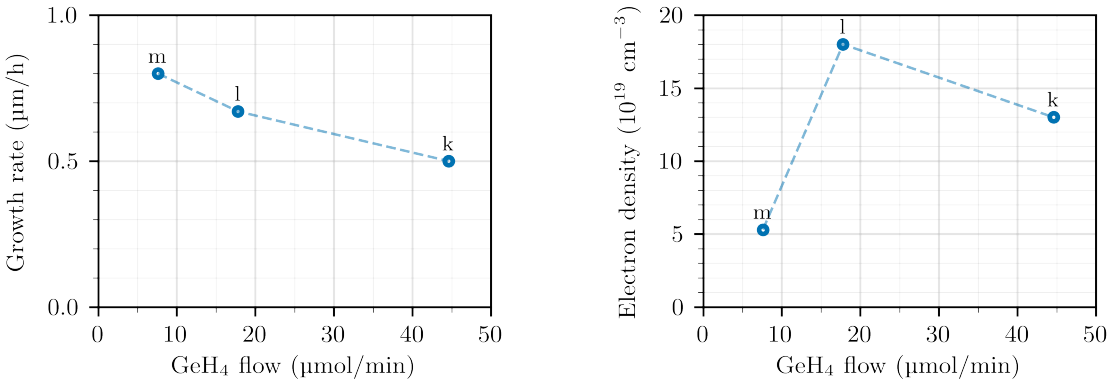

Figure 3. GR and electrons density for GaN:Ge layers grown at the TMGa flow of 25 mol/min, as a function of GeH_4 flow.

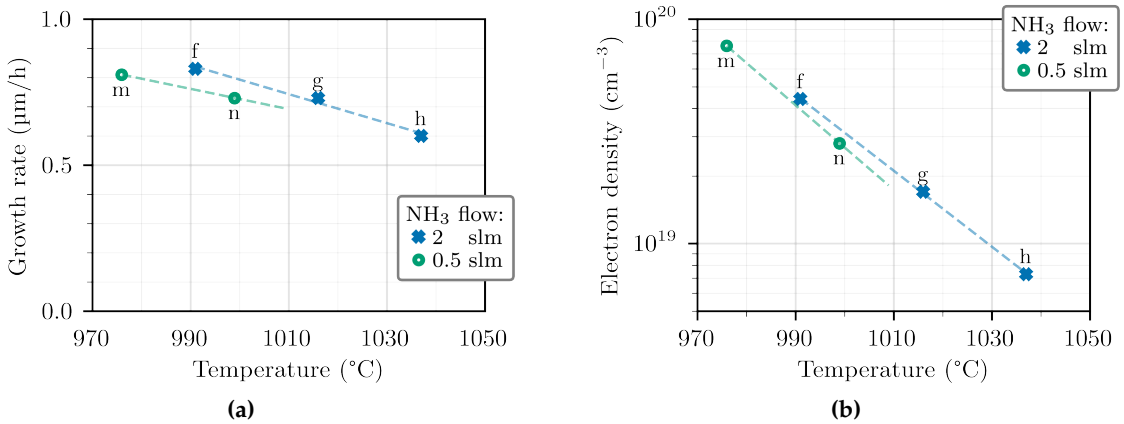

Figure 4. Density of free electrons in GaN:Ge layers grown at different temperatures and NH_3 flows, while the TMGa and GeH_4 flows are kept at 26.8 and 7.5 mol/min, respectively.

Preprints (www.preprints.org) | NOT PEER-REVIEWED | Posted: 28 December 2020 doi:10.20944/preprints202012.0678.v1

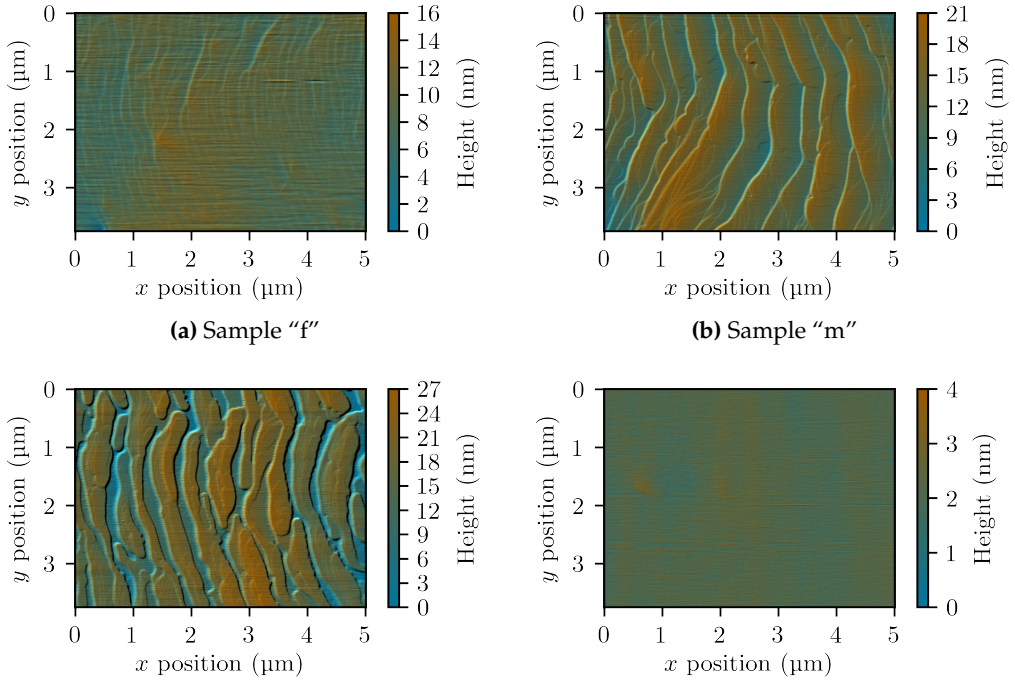

(a) Sample "f" **(b)** Sample "m"

(c) Sample "k" **(d)** Sample "m" after MCP

Figure 5. Atomic-force microscopy (AFM) scans of four GaN:Ge layers. Subfigure d shows the same sample as subfigure b but after mechano-chemical polishing (MCP).

4. Surface morphology

A remarkable difference between the first and the second series of samples (grown with a NH_3 flow of 2 slm and 0.5 slm, respectively) resides in the surface morphology. This was analyzed by optical microscopy and atomic-force microscopy (AFM). The samples of the first series, with the only exception of those grown at temperatures above 1050C (i.e. samples "d" and "e"), are characterized by the presence of V-pits with a density of 10^7 cm^{-2}. The size of the V-pits tends to decrease as the temperature approaches 1050C, by which they disappear completely. Unfortunately, as was discussed above, it is not possible to incorporate a satisfactory amount of germanium dopant when growing at temperature higher than 1050C. Aside of the V-pits, the surface appears otherwise flat, and growth steps are clearly visible in the AFM scans such as the one shown in Figure 5a.

On the other hand, the samples of the second series are strongly affected by step bunching. Instead of individual atomic steps, fewer but higher macrosteps are observed in AFM scans, as can be seen of sample "m" shown in Figure 5b (for this scan, an area without V-pits was accurately chosen). Moreover, the macrostep height depends on the germanium concentration. Comparing samples "m" and "k" in Figures 5b and 5c, one can note that the height of the macrosteps increases as the GeH_4 flow is increased from 7.6 mol/min to 45 mol/min. To make a quantitative comparison possible, sections of all the AFM scans in Figure 5 performed along the x-axis are shown in Figure 6. It can be observed that the macrostep height increases from 8 nm to 15 nm, corresponding to about 30 and 60 monolayers, respectively. However, no V-pits were found in the samples of the second series. In our experience, the lack of V-pits in samples grown at low temperature is always connected to the emergence of step bunching. Once again, a similar case where the lowering of the NH_3 flow produced a significant change of the growth morphology was observed in InGaN layers [21].

While step bunching is certainly not a desirable feature by itself, in this case it can prove useful in that it blocks V-pit formation. A good reason to prefer step bunching to V-pits is because the affected layer can be planarized more easily, for example by overgrowing with a high-temperature GaN layer, or by mechano-chemical polishing (MCP). To prove this, sample "m" was treated with a

Preprints (www.preprints.org) | NOT PEER-REVIEWED | Posted: 28 December 2020 doi:10.20944/preprints202012.0678.v1

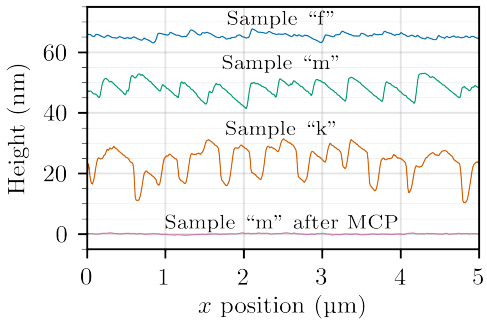

Figure 6. Section along the x-axis of the scans shown in Figure 5. The graphs have been displaced vertically so that they would not overlap each other.

10-minute-long MCP process, by which we estimate that approximately 100 nm were etched. The AFM scan of the resulting flat surface is shown in Figure 5d. We believe that the same result could likely be obtained with a shorter MCP run as well.

5. Final remarks

The effect of growth temperature and precursor flows on germanium incorporation and surface morphology was studied in depth. A total of 14 samples with GaN:Ge layers were grown and characterized. It was found that the germanium incorporation depends on the growth conditions in a similar way to indium incorporation in InGaN layers, namely it increases at low temperature, high growth rate and high V/III ratio, whereas it does not increase linearly with the precursor flow but instead it saturates and then it slowly decreases. The effect of pressure was not tested but, based on the behavior of indium, one can expect that the incorporation of germanium would increase when the pressure is low [22]. The samples of our second series, grown with a reduced NH_3 flow, were affected by step bunching but were also free of V-pits. Within the first series, instead, only samples "d" and "e" were also lacking V-pits, however they also incorporated considerably less germanium because of the high temperature of growth. The macrosteps produced by step bunching are of course undesirable but we showed that they can at least be removed by a quick 10-minute MCP process. As for the electron mobility in our GaN:Ge layers, it is about as high as the other values reported in the literature (see Figure 7), so there can be little doubt as to the quality of our samples.

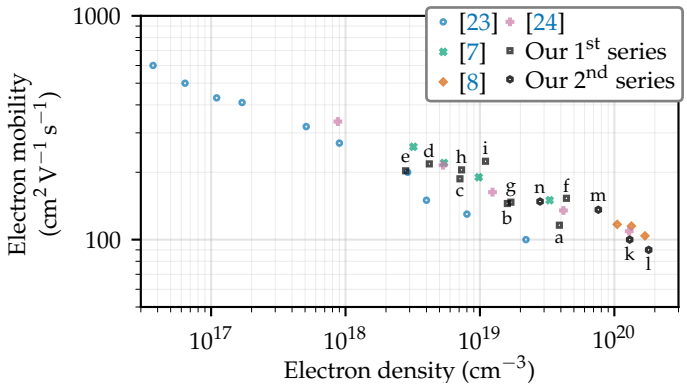

Figure 7. The electron mobility of all samples as a function of the electron density and compared to equivalent values from the literature.

Funding: This research was funded by the Polish National Centre for Science via the MINIATURA grant number 2019/03/X/ST5/01907.

Conflicts of Interest: The authors declare no conflict of interest.

References

1. Arcara, V.F.; Damilano, B.; Feuillet, G.; Vézian, S.; Ayadi, K.; Chenot, S.; Duboz, J.Y. Ge doped GaN and $Al_{0.5}Ga_{0.5}N$-based tunnel junctions on top of visible and UV light emitting diodes. *J. Appl. Phys.* **2019**, *126*, 224503. doi:10.1063/1.5121379.
2. Stanczyk, S.; Czyszanowski, T.; Kafar, A.; Czernecki, R.; Targowski, G.; Leszczynski, M.; Suski, T.; Kucharski, R.; Perlin, P. InGaN laser diodes with reduced AlGaN cladding thickness fabricated on GaN plasmonic substrate. *Appl. Phys. Lett.* **2013**, *102*, 151102. doi:10.1063/1.4801949.
3. Fritze, S.; Dadgar, A.; Witte, H.; Bügler, M.; Rohrbeck, A.; Bläsing, J.; Hoffmann, A.; Krost, A. High Si and Ge n-type doping of GaN doping—Limits and impact on stress. *Appl. Phys. Lett.* **2012**, *100*, 122104. doi:10.1063/1.3695172.
4. Markurt, T.; Lymperakis, L.; Neugebauer, J.; Drechsel, P.; Stauss, P.; Schulz, T.; Remmele, T.; Grillo, V.; Rotunno, E.; Albrecht, M. Blocking Growth by an Electrically Active Subsurface Layer: The Effect of Si as an Antisurfactant in the Growth of GaN. *Phys. Rev. Lett.* **2013**, *110*, 036103. doi:10.1103/PhysRevLett.110.036103.
5. Götz, W.; Kern, R.S.; Chen, C.H.; Liu, H.; Steigerwald, D.A.; Fletcher, R.M. Hall-effect characterization of III–V nitride semiconductors for high efficiency light emitting diodes. *Mater. Sci. Eng. C* **1999**, *59*, 211–217. doi:10.1016/S0921-5107(98)00393-6.
6. Wang, H.; Chen, A.B. Calculation of shallow donor levels in GaN. *J. Appl. Phys.* **2000**, *87*, 7859. doi:10.1063/1.373467.
7. Oshima, Y.; Yoshida, T.; Watanabe, K.; Mishima, T. Properties of Ge-doped, high-quality bulk GaN crystals fabricated by hydride vapor phase epitaxy. *J. Cryst. Growth* **2010**, *312*, 3569–3573. doi:10.1016/j.jcrysgro.2010.09.036.
8. Wieneke, M.; Witte, H.; Lange, K.; Feneberg, M.; Dadgar, A.; Bläsing, J.; Goldhahn, R.; Krost, A. Ge as a surfactant in metal-organic vapor phase epitaxy growth of a-plane GaN exceeding carrier concentrations of 10^{20} cm^{-3}. *Appl. Phys. Lett.* **2013**, *103*, 012103. doi:10.1063/1.4812666.
9. Perlin, P.; .; Holc, K.; Sarzyński, M.; Scheibenzuber, W.; Łucja Marona.; Czernecki, R.; Leszczyński, M.; Bockowski, M.; Grzegory, I.; Porowski, S.; Cywiński, G.; Firek, P.; Szmidt, J.; Schwarz, U.; Suski, T. Application of a composite plasmonic substrate for the suppression of an electromagnetic mode leakage in InGaN laser diodes. *Appl. Phys. Lett.* **2009**, *95*, 261108. doi:10.1063/1.3280055.
10. Kirste, R.; Hoffmann, M.P.; Sachet, E.; Bobea, M.; Bryan, Z.; Bryan, I.; Nenstiel, C.; Hoffmann, A.; Maria, J.P.; Collazo, R.; Sitar, Z. Ge doped GaN with controllable high carrier concentration for plasmonic applications. *Appl. Phys. Lett.* **2013**, *103*, 242107. doi:10.1063/1.4848555.
11. Kim, I.H.; Park, H.S.; Park, Y.J.; Kim, T. Formation of V-shaped pits in InGaN/GaN multiquantum wells and bulk InGaN films. *Appl. Phys. Lett.* **1998**, *73*, 1634. doi:10.1063/1.122229.
12. Iwinska, M.; Takekawa, N.; Ivanov, V.Y.; Amilusik, M.; Kruszewski, P.; Piotrzkowski, R.; Litwin-Staszewska, E.; Lucznik, B.; Fijalkowski, M.; Sochacki, T.; Teisseyre, H.; Murakami, H.; Bockowski, M. Crystal growth of HVPE-GaN doped with germanium. *J. Cryst. Growth* **2017**, *480*, 102–107. doi:10.1016/j.jcrysgro.2017.10.016.
13. Zhang, Y.; Wang, J.; Su, X.; Cai, D.; Xu, Y.; Wang, M.; Hu, X.; Zheng, S.; Xu, L.; Xu, K. Investigation of pits in Ge-doped GaN grown by HVPE. *Jpn. J. Appl. Phys.* **2019**, *58*, 120910. doi:10.7567/1347-4065/ab56f5.
14. Bogusławski, P.; Bernholc, J. Doping properties of C, Si, and Ge impurities in GaN and AlN. *Phys. Rev. B* **1997**, *56*, 9496. doi:10.1103/PhysRevB.56.9496.
15. Chen, C.H.; Liu, H.; Steigerwald, D.; Imler, W.; Kuo, C.P.; Craford, M.G.; Ludowise, M.; Lester, S.; Amano, J. A study of parasitic reactions between NH3 and TMGa or TMAl. *J. Electron. Mater.* **1996**, *25*, 1004–1008. doi:10.1007/BF02666736.
16. Koleske, D.D.; Wickenden, A.E.; Henry, R.L.; Culbertson, J.C.; Twigg, M.E. GaN decomposition in H2 and N2 at MOVPE temperatures and pressures. *J. Cryst. Growth* **2001**, *223*, 466–483. doi:10.1016/S0022-0248(01)00617-0.
17. Piner, E.L.; McIntosh, F.G.; Roberts, J.C.; Boutros, K.S.; Aumer, M.E.; Joshkin, V.A.; El-Masry, N.A.; Bedair, S.M.; Liu, S.X. A Model for Indium Incorporation in the Growth of InGaN Films. *Mater. Res. Soc. Symp. Proc.* **1997**, *449*, 85–88. doi:10.1557/PROC-449-85.
18. Matsuoka, T.; Yoshimoto, N.; Sasaki, T.; Katsui, A. Wide-gap semiconductor InGaN and InGaAln grown by MOVPE. *J. Electron. Mater.* **1992**, *21*, 157–163. doi:10.1007/BF02655831.

19. Ou, J.; Chen, W.K.; Lin, H.C.; Pan, Y.C.; Lee, M.C. An Elucidation of Solid Incorporation of InGaN Grownby Metalorganic Vapor Phase Epitaxy. *Jpn. J. Appl. Phys.* **1998**, *37*, L633–L636. doi:10.1143/JJAP.37.L633.
20. Guo, Y.; Liu, X.L.; Song, H.P.; Yang, A.L.; Xu, X.Q.; Zheng, G.L.; Wei, H.Y.; Yang, S.Y.; Zhu, Q.S.; Wang, Z.G. A study of indium incorporation in In-rich InGaN grown by MOVPE. *Appl. Surf. Sci.* **2010**, *256*, 3352–3356. doi:10.1016/j.apsusc.2009.11.081.
21. Oliver, R.A.; Kappers, M.J.; Humphreys, C.J.; Briggs, G.A.D. The influence of ammonia on the growth mode in InGaN/GaNheteroepitaxy. *J. Cryst. Growth* **2004**, *272*, 393–399. doi:10.1016/j.jcrysgro.2004.08.072.
22. Kim, D.J.; Moon, Y.T.; Song, K.M.; Lee, I.H.; Park, S.J. Effect of Growth Pressure on Indium Incorporation During the Growth of InGaN by MOCVD. *J. Electron. Mater.* **2001**, *30*, 99–102. doi:10.1007/s11664-001-0107-y.
23. Nakamura, S.; Mukai, T.M.T.; Senoh, M.S.M. Si- and Ge-Doped GaN Films Grown with GaN Buffer Layers. *Jpn. J. Appl. Phys.* **1992**, *31*, 2883. doi:10.1143/JJAP.31.2883.
24. Young, N.G.; Farrell, R.M.; Iza, M.; Nakamura, S.; DenBaars, S.P.; Weisbuch, C.; Speck, J.S. Germanium doping of GaN by metalorganic chemical vapor deposition for polarization screening applications. *J. Cryst. Growth* **2016**, *455*, 105–110. doi:10.1016/j.jcrysgro.2016.09.074.